

# TRACKING SIMULATIONS AND DYNAMIC MULTIPOLE SHIMMING FOR HELICAL UNDULATORS \*

J. Bahrtdt, M. Scheer, G. Wüstefeld <sup>1</sup>, BESSY, Berlin, Germany

## Abstract

Beam dynamic effects of an APPLE II type undulator in the BESSY II storage ring are simulated. The fast simulation method is based on a multiple harmonic decomposition of the magnetic field and a generating function tracking approach. Because of the relatively large undulator period length of 112 mm corrections of the dynamic multipoles using so called L-shims are required to maintain a good dynamical aperture.

## INTRODUCTION

There is an increasing demand on operating helical insertion devices (ID) as sources of polarized synchrotron radiation. The influence of such IDs, specially of the APPLE II [1] type, on the beam dynamics in the 1.7 GeV BESSY II ring is discussed in this paper, together with the applied simulation tools. The results are valid for an idealized ID model to check intrinsic effects of the ID on the beam dynamics. A sequence of identical periods is sufficient to model the full ID. The developed methods are applied to optimize dynamical multipole correctors (L-shims) of the ID, the beam working point and harmonic sextupoles.

The paper discusses three topics, (i) the harmonic scalar potential expansion and dynamic multipole correction, (ii) the generating function (GF) based tracking routine [2], and (iii) some beam dynamic results. A frequency map method is applied to analyze tracking data. The tracking results apply only to the horizontal and vertical planar wiggle mode of integer, multiple periods in the ID, obtained by tuning the ID shift parameter  $\psi$  to 0 and  $\pi$  radian, respectively. These constraints result in a significant simplification of the GF tracking routine. However, the method is sufficiently general to be extended to arbitrary shift parameters and end pole shaping [3]. In our present example, an explicit end pole correction is not required. The  $\psi = \pi$  mode is probably the most critical tuning case for the beam dynamics, as expected from the fast changing field shape shown in Fig. 1. Most of the results apply for this case.

An ideal ID has vanishing horizontal and vertical field integrals, integrated along straight lines parallel to the ID axis. Because electrons will not follow these lines but wiggle around it, they accumulate integrated orbit kicks and shifts. These orbit distortions are described by dynamical multipoles [4]. The relatively large period length of 112 mm of the studied ID UE112 [1] together with the moderate beam energy of 1.7 GeV leads to relatively large orbit wiggles, enhancing the impact of dynamical multipoles. As

the result of this study, we suggest appropriate field shims (L-shims) to cancel the dynamical multipoles [1, 5, 6]. In this way, a large horizontal beam acceptance can be preserved.

## HARMONIC FIELD EXPANSION

An APPLE II undulator is composed of four identical magnet rows which can be moved longitudinally with respect to each other. The vertical field distribution of one row as derived from a numerical simulation is decomposed into  $2 \times 20$  Fourier components. Using these coefficients the complete 3D-field distribution is obtained from the scalar potential,

$$V = \sum_{n=1}^N (V_{1n} + V_{2n} + V_{3n} + V_{4n})$$

$$V_{1n} = \left( \frac{e^{nk_y y}}{nk_y} (B_{cn} c_{xn-} + B_{sn} s_{xn-}) + B_0 \frac{e^{k_z z}}{Nk_z} \right) c_{z+}$$

$$c_{xn\pm} = \cos(nk_x (x \pm x_0))$$

$$s_{xn\pm} = \sin(nk_x (x \pm x_0))$$

$$c_{z\pm} = \cos(k_z z \pm \psi/2).$$

The terms  $V_{2n}$ ,  $V_{3n}$  and  $V_{4n}$  are constructed by obvious symmetry operations. Similarly, the vertical field integral distribution of the row phase  $\psi$  dependent terms of the L-shims is Fourier expanded and the analytical representation has the form:

$$\tilde{V} = \sum_{n=1}^N \tilde{V}_n$$

$$\tilde{V}_n = \frac{1}{nk_y} (\tilde{B}_{c1n} \cos(nk_x x) + \tilde{B}_{s1n} \sin(nk_x x)) e^{nk_y y} + \frac{1}{nk_y} (\tilde{B}_{c2n} \cos(nk_x x) + \tilde{B}_{s2n} \sin(nk_x x)) e^{-nk_y y}$$

Generally, the coefficients for the upper and lower magnet girder may be different though for the UE112 case we applied a symmetric configuration.

The field  $V$  and the z-integrated field  $\tilde{V}$  parameterization with only  $2 \times 20$  coefficients reproduces the real distribution in three dimension for various gaps and row phases with a high accuracy, Fig. 1. The dynamical multipoles and the field due to the iron shims depend on the row phase  $\psi$ , and they are roughly proportional to each other [5].

## GENERATING FUNCTION

The tracking routine is based on an analytic, expanded form of the GF in a Cartesian coordinate system [2]. A GF

\*Funding: Bundesministerium fuer Bildung und Forschung and the Land Berlin.

<sup>1</sup>Author: wuestefeld at bessy.de

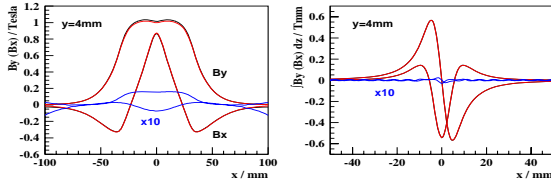


Figure 1: Comparison of simulated fields (black) and fields generated from the analytical model (red). The differences (blue) are enhanced by a factor of ten. Left: vertical  $B_y$  ( $\psi = 0$ ) and horizontal  $B_x$  ( $\psi = \pi$ ) UE112 field. Right: Horizontal and vertical field integral changes due to 4 L-shims for  $\psi = \pi$ .

of type ' $F_3$ ' is approximated by an iterative solution of the Hamilton Jacobi equation [7, 8],  $H + \partial F/\partial z = 0$ . The Hamiltonian is expanded as,

$$H = 1 + (P_x - A_x)^2/2 + (P_y - A_y)^2/2.$$

The vector potentials are normalized by  $B\rho$  of the actual electron momentum and are derived from the scalar potentials  $V$  with  $A_z=0$ . The result of the 2<sup>nd</sup> order expansion is equivalent to a direct integration of the Hamiltonian over one full period,

$$F_3 = f_{101}p_{xf} + f_{011}p_{yf} + f_{002} \\ -z - x_i p_{xf} - y_i p_{yf} - p_{xf}^2 z/2 - p_{yf}^2 z/2,$$

where the coordinates at the entrance point into the ID period are  $(x_i, p_{xi}, y_i, p_{yi})$  and at the exit point  $(x_f, p_{xf}, y_f, p_{yf})$ . For the  $f_{abc}$  terms we get

$$-2f_{002} = \int (A_x^2 + A_y^2) dz.$$

The values of  $f_{101} = \int A_x dz$  and  $f_{011} = \int A_y dz$  are zero in the examples discussed here (not necessary for the applied method), equivalent to vanishing 2<sup>nd</sup> field integrals, e.g.  $\int \int B_y dz dz = 0$ .

The conjugate, mixed coordinates are given by applying the relations

$$\partial F_3/\partial p_{xf} = -x_f, \quad \partial F_3/\partial p_{yf} = -y_f, \\ \partial F_3/\partial x_i = -p_{xi}, \quad \partial F_3/\partial y_i = -p_{yi}.$$

At this level of approximation the implicit coordinate relations can directly be solved from the GF.

A comparison between our idealized model and the program code 'WAVE' [9], based on finite integral methods for the field and the particle tracking, of the unshimmed, full device including end poles is presented in Figs. 2 and 3, for  $\psi = \pi$ . Fig.2 shows the difference between all 4 entrance and exit coordinates. The initial horizontal coordinates are evenly distributed on a horizontal phase space ellipse with  $y=5\text{mm}$  fixed. Therefore, each initial position  $x_i$  value is correlated with two equal, initial  $x'_i$ -values of opposite sign. The difference of these coordinates  $\Delta x = x_f - x_i$ , e.g.,

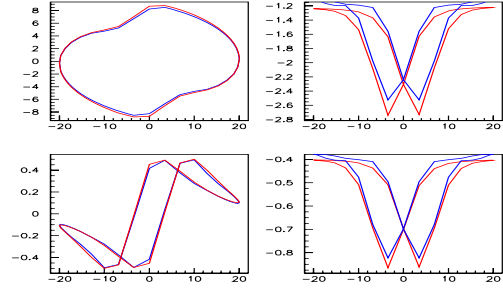


Figure 2: Comparison of GF based simulation of the full device (blue) with the symplectic integration code 'WAVE' (red). The difference between exit and entrance coordinates (clock wise, starting upper figure left)  $\Delta x$ ,  $\Delta x'$ ,  $\Delta y'$  and  $\Delta y$  are plotted versus the horizontal entrance point, axes are in mm and mrad.

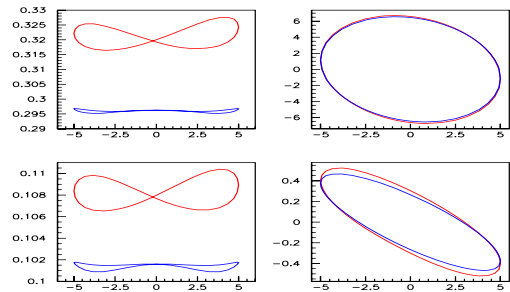


Figure 3: Same as Fig.2, but starting coordinates are varied along a vertical phase space ellipse and plotted versus the vertical entrance points in mm.

after passing the ID is shown in the figure, calculated by the GF and by WAVE. Similarly in Fig. 3 the vertical coordinates are evenly distributed on a vertical phase space ellipse with  $x=20\text{mm}$  fixed. The agreement is in general very good, beside a position offset visible in Fig. 3.

## TRACKING RESULTS

For the optics simulation a 6x6 tracking code is written. Sextupoles and rf-cavity are simple kick elements. The dipoles are simulated in second order, applying the MAD method as described in [10]. The GF for the insertion device is included.

A correction method for the UE112 is required to suppress the effect of the dynamic multipoles. This is simulated by L-shims, placed between each second period as 2-dim field kicks. The effect of the shims is shown in Fig. 4, where the integrated kick accumulated by an electron per passage of the ID in the horizontal plane is shown. The initial horizontal phase space positions are distributed on an ellipse of 30 mm and 1.87 mrad axes. The unshimmed case leads to large kicks of different signs for particles starting

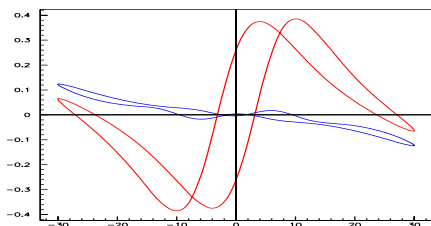


Figure 4: Horizontal kick in mrad per ID an electron receives as a function of horizontal displacement in mm. Blue with shims, red: no shims.

with, e.g.,  $x_i = 0$  and  $x'_i$ -values of opposite signs. The shimmed case shows a strongly reduced kick strength. If unshimmed, the ID shows very nonlinear kicks.

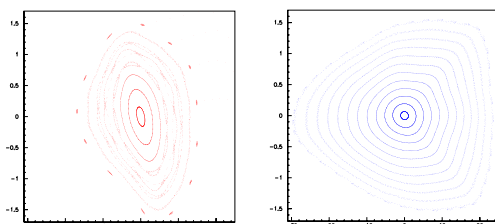


Figure 5: Horizontal phase space plot of 1000 turns and increasing horizontal starting amplitude at nominal momentum. The vertical starting amplitude is always 1 mm. Left: unshimmed case, right: shimmed case.

An example of the horizontal phase space is shown in Fig. 5, with and without shim corrections. The shimming leads to a gain in stable horizontal phase space, extending to 30 mm. Without shims only half the range is stable. In this simulation the starting value in the vertical plane was 1 mm. Derived from a frequency map analysis, shown in Fig. 6, it seems to be advantageous, to slightly tune the harmonic sextupoles to keep the tune spread caused by the ID small. If unshimmed, the dynamical multipoles lead to an intolerable large tune spread, already at half of the required dynamic aperture. The working point was adjusted to avoid major resonances. Finally, the correction results in a stable dynamic aperture within the requested area. Including the shims, the induced, small amplitude tune shift for  $\psi = \pi$  is less than 0.02 in both planes (ID on/off).

We acknowledge the fruitful discussion with our colleagues J. Feikes, A. Gaup, P. Kuske and W. Frentrop.

## REFERENCES

- [1] J. Bahrtdt et al., 'Preparing The BESSY APPLE Undulators For Topping Up Operation', Proc. SRI 2006, Daegu (Korea).
- [2] G. Wüstefeld, J. Bahrtdt, 'Canonical Particle Tracking in Undulator Fields', Proc. PAC 1991, San Francisco (USA), p. 266.

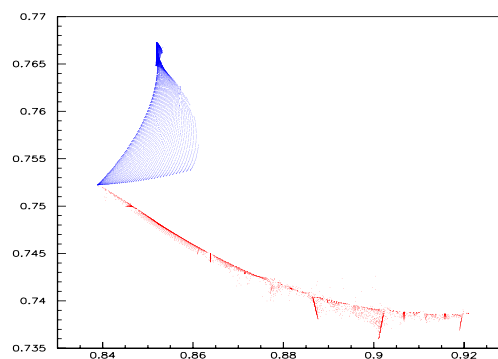


Figure 6: Frequency map  $\Delta Q_y / \Delta Q_x$  at the nominal momentum. The max. horizontal amplitudes are less than 30 mm and max. vertical amplitudes are less than 5 mm. Dynamical multipoles shimmed (blue) and unshimmed (red).

- [3] G. Wüstefeld, M. Scheer, 'Canonical Particle Tracking and End Pole Matching of Helical Insertion Devices', Proc. PAC 1997, Vancouver (Canada), p. 1418.
- [4] J. Safranek et al, 'Nonlinear dynamics in a SPEAR wiggler', Phys. Rev. ST Accel. Beams 5, 010701 (2002).
- [5] J. Chavanne et al., 'Recent Achievements and Future Prospects of ID Activities at the ESRF', Proc. EPAC 2000, Vienna (Austria), p. 2346.
- [6] P. Kuske, 'Effects of Fringe Fields and Insertion Devices Revealed Through Experimental Frequency Map Analysis', Proc. PAC 2005, Knoxville (USA), p. 266.
- [7] H. Goldstein, 'Klassische Mechanik', Akademische Verlagsgesellschaft, Frankfurt, 1963, p. 303.
- [8] G. Wüstefeld, 'Particle Tracking with Generating Functions of Magnetic Fringing Fields', Proc. PAC 1995, Dallas (USA), p. 2868.
- [9] M. Scheer, 'WAVE', BESSY, computer code.
- [10] F.Ch. Iselin, 'The MAD program', 'Physical Methods Manual', CERN/SL/92 (AP), p. 15, 1994.